Department of Mechanical Engineering

Adaptive Equivalent Circuit Models for Battery Management Systems of Lithium-ion Battery Degradation – A Review

Literature Research Project (LRP)

Joshua Ho

Abstract

Lithium-ion battery degradation presents a fundamental challenge for battery management systems (BMS), as ageing progressively reduces capacity, power capability, and safety while remaining largely unobservable through direct sensing. Equivalent circuit models (ECMs) are therefore widely adopted due to their computational efficiency, yet conventional lumped formulations exhibit weak physical correspondence and limited ability to represent degradation-dependent internal states, motivating the need for a comprehensive review.

This review critically examines the evolution of adaptive ECMs for degradation-aware BMS applications, synthesising developments across integer- and fractional-order lumped circuits, physics-informed extensions, and adaptive identification frameworks. A unifying taxonomy is proposed that distinguishes structurally physics-informed ECMs (SPI-ECMs), whose topology is derived from reduced-order discretization of first-principles electrochemical models, from parametrically physics-informed ECMs (PPI-ECMs), where physical meaning arises through constrained parameter evolution. Using this framework, the review shows that while SPI-ECMs provide superior physical causality and spatial resolution, their computational and identifiability burdens limit robustness as degradation progresses. Both SPI-ECMs and PPI-ECMs demonstrate advances in modelling SEI growth, lithium plating, and dendrite formation, whereas particle cracking remains unrepresented within existing ECM structures. The physical interpretability of fractional-order elements, particularly the constant phase element, also remains poorly understood despite widespread use. By reviewing major adaptive algorithm families and experimental techniques, onboard real-time EIS, including research into dynamic EIS, is identified as a key enabler for next-generation physics-informed ECMs. Further, the review demonstrates the natural trade-off between computational efficiency and model accuracy, and that ECM evaluation frameworks must be grounded in explicit deployment constraints and tighter integration with onboard sensing and cloud-integration.

Objectives

This LRP aim to address the following research questions:

1. What degradation modes and mechanism govern the ageing of lithium-ion batteries?
2. How have equivalent-circuit model architectures evolved historically, and how has this evolution improved their ability to represent degradation-related internal states?
3. What adaptive identification techniques have been developed to estimate ECM parameters and states?
4. To what extent are existing adaptive ECMs fit-for-purpose and what research gaps and opportunity remain for improving future degradation-aware modelling?

Referencing Styles

All citations and references adhere to the IEEE referencing standard

Contents

1 Introduction

The rapid proliferation of lithium-ion batteries (LIBs) as sources of energy and storage has brought battery degradation into sharp focus, due to concerns over its economic viability, safety, and sustainability. As LIBs age, degradation processes lead to progressively reducing power and capacity [1]. These changes do not compromise fast charging, thermal stability, state estimation, and lifespan. Fortunately, this can be mitigated by appropriate oversight from estimations during LIB operation, using battery management systems (BMS). The general framework of operation is illustrated in Figure 1.

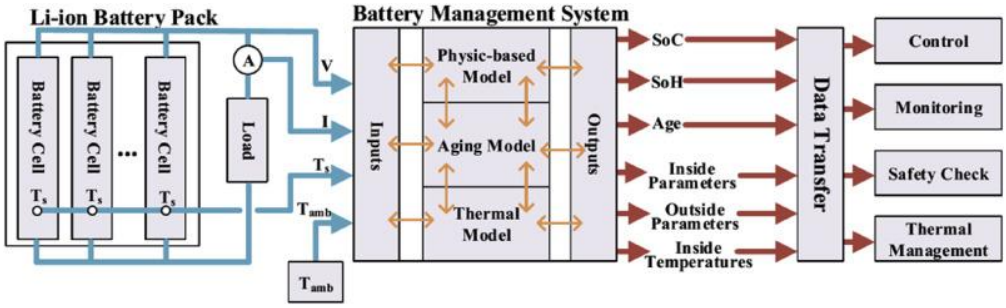

Figure 1. Schematic of BMS inputs, outputs and applications

BMS rely heavily on internal states such as state of charge (SOC), state of health (SOH) and state of power (SOP) to regulate charge/discharge control, optimise power delivery, and prevent operation outside safe limits. However, these states are not directly measurable and must instead be inferred from voltage, current, and temperature measurements. This has made battery modelling central to modern BMS design.

Industry BMSs largely rely on equivalent circuit models (ECMs), which are computationally efficient but offer limited physical interpretability and poor generalisability across chemistries and ageing states. Physics-based models (PBMs) provide far richer descriptions of electrochemical and transport phenomena but are too computationally intensive for real-time use [2]. This gap has led to physics-informed ECMs (PI-ECMs), which seek to preserve ECM efficiency while introducing physically meaningful, state-dependent behaviour.

The literature surrounding PI-ECMs has grown rapidly, but definitions are inconsistent and often conflate structurally derived circuit networks with empirically structured circuits whose physical meaning arises through parameter evolution. Likewise, while many studies propose adaptive identification algorithms, their relationship to specific degradation modes is seldom articulated. The original contribution of this review is therefore two-fold: (i) it introduces a clear taxonomy distinguishing structurally physics-informed (SPI-ECMs) from

parametrically physics-informed ECMs (PPI-ECMs), resolving ambiguity and enabling more consistent evaluation, and (ii) it frames the evolution of ECM architectures and adaptive algorithms explicitly through the lens of degradation observability, clarifying how different modelling approaches reveal ageing mechanisms relevant to BMS decisions.

2 LIB Fundamentals

2.1 LIB Basic Structure and Operation

Lithium-ion batteries (LIBs) are composite electrochemical systems comprising positive and negative electrodes coated onto metallic current collectors, a porous separator, and an ion-conducting electrolyte that also supplies mobile Li^+ species (Figure 2). Together, these components enable reversible redox reactions during charge and discharge [1]. The positive electrode (PE), which is typically a lithium transition-metal oxide, largely determines the cell's energy density. The negative electrode (NE), commonly graphite, graphite-silicon blends, or lithium titanate, intercalates Li^+ during charge and releases it during discharge. When a cell is charged, Li^+ deintercalates from the PE and migrates through the electrolyte and separator to the NE, while electrons flow through the external circuit; discharge reverses this process, leading to a "rocking chair motion" [1].

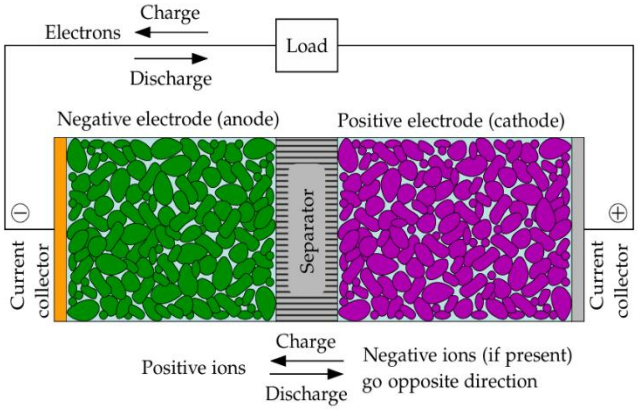

Figure 2. Schematic diagram of a lithium-ion cell. Source: [6]

2.2 LIB Degradation

Lithium-ion battery ageing arises from stressors such as cycling, temperature, SOC, and current load, which activate underlying degradation mechanisms. Following Edge and O'Kane [1], degradation is organised hierarchically into mechanisms (physicochemical processes), modes (their thermodynamic or kinetic consequences), and effects (measurable outcomes). This structure enables later mapping between physical degradation and model parameters.

Ageing in LIBs is dominated by four modes, loss of lithium inventory (LLI), loss of active material (LAM), impedance rise, and stoichiometric drift, each linked to a small set of well-established mechanisms. SEI growth consumes cyclable lithium and increases interfacial resistance, accelerating under high temperature, high SOC, or high current. Lithium plating

occurs when anode overpotential becomes sufficiently negative, producing metallic deposits that may become “dead lithium,” enhance SEI formation, and, in extreme cases, form dendrites. Particle fracture, driven by repeated lithiation-induced strain, isolates regions of active material and exposes fresh surfaces that further promote parasitic reactions. These tightly coupled mechanisms and modes remain central to ongoing efforts in degradation modelling, diagnosis, and prognosis.

3 Modelling LIBs with ECMs

Many LIB states and internal parameters are not directly measurable by sensor. Therefore, equivalent circuit models (ECMs) were introduced as electrical analogues of the cell, useful for online state estimations. Lumped ECMs are first discussed, followed by physics-informed ECMs. The models are first introduced, followed by a discussion of their usefulness in degradation and ageing.

3.1 Lumped ECMs

Lumped ECMs are the earliest approaches to model LIBs. They assume that the entire electrode domain can be collapsed into a few lumped elements, making no explicit distinction between anode and cathode processes or spatial variations across the cell. Their strength lies in its simplicity and speed of parameterisation, low computational burden, and straightforward integration into BMS algorithms. Lumped ECMs are broadly divided into integer-order ECM and fractional-order ECM.

3.1.1 Integer-order ECMs

Integer-order ECMs use a voltage source, resistor, capacitors and inductors as circuit elements. Some examples with their respective output equations are listed in Figure 3.

The Rint model represents a cell as an ideal voltage source with a single series resistance, enabling fast resistance estimation from OCV–SOC data and simple pack-level simulations. Its linear structure cannot capture polarisation or diffusion effects, making it unsuitable for detailed cell modelling, but its simplicity remains useful for basic electrical analyses.

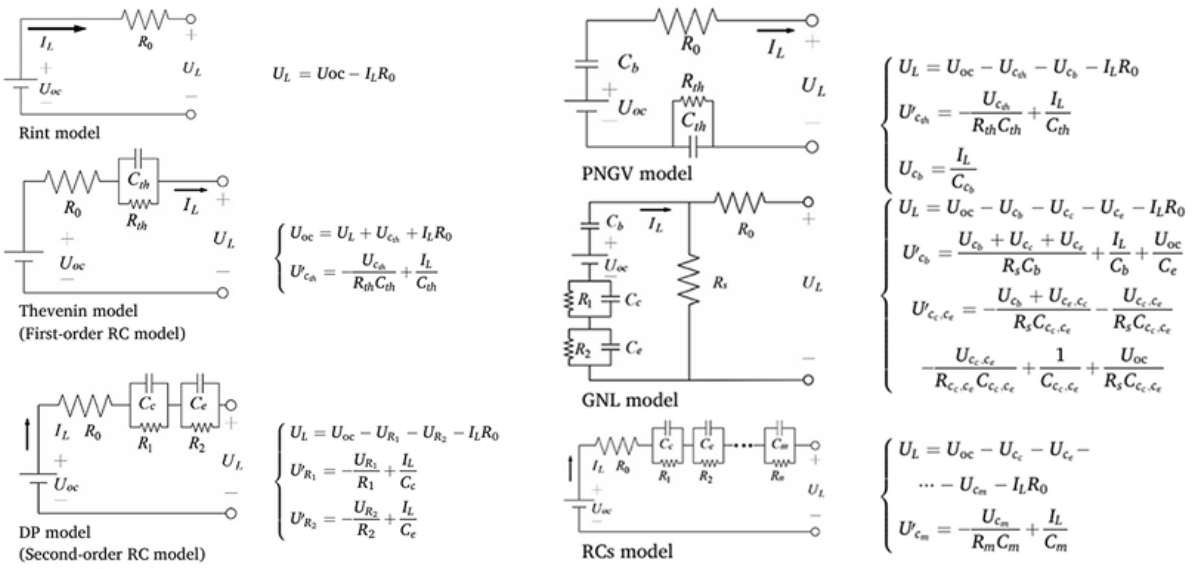

Figure 3. Commonly Used Lumped ECM for LIBs. Adapted from ref. [4]

Over time, ECMs expanded to the Thevenin (first-order RC) model, which adds an RC parallel circuit composed of charge transfer resistance R_{ct} and capacitance C_e to the Rint model, simulating diffusion during charge and discharge. Despite its simple structure, it is still widely used in academia and industry. The DP model (second-order RC model) adds another RC parallel network to the Thevenin model, separating simulations of electrochemical polarization and concentration polarization during battery cycling. It is possible to increase the number of RC terms with the motivation of identifying other physical phenomena such as charge transfer and double layer effects [3], yet it does not necessarily improve model fidelity but could instead lead to higher overfitting chances and computational demand, and in short, diminishing returns [4]. Thus, the number of RC pairs selected should be determined on a case-by-case basis.

The PNGV model [5], originally created for standardizing the test procedure for battery instantaneous peak power, adds a series capacitance C_Q to describe how OCV evolves with cycling. Its design also allows state of power (SOP) estimations. The GNL model combines the benefits of the aforementioned, with the addition of self-discharge factors, by adding a dedicated self-discharge resistance branch in parallel with the main ohmic path and polarization network in the ECM. Both PNGV and GNL model despite having its benefits, introduces structural complexity, and thus requires stricter calibration.

The enhanced self-correcting (ESC) model, popularized by Plett [6] further extends this family by incorporating a hysteresis state to the Thevenin model as shown in Figure 4a, allowing the ECM to capture asymmetry between charge and discharge voltage trajectories and to improve model robustness, that is, the model's ability to handle

uncertainties and identify its own errors. The total hysteresis voltage at discretized time steps is given by

$$v_h[k] = M_0 s[k] + Mh[k]$$

where the first term $M_0 s[k]$ represents the instantaneous, sign-dependent hysteresis jump $h_i[k]$, the second term $Mh[k]$ describes the SOC-dependent hysteresis that evolves over time. The fitness of the model (in orange) is illustrated, by overlaying on top of the experimental results (in blue) in Figure 4b, showing consistency, despite inaccuracies prior to voltage plateau and major deviations at extreme SOC levels.

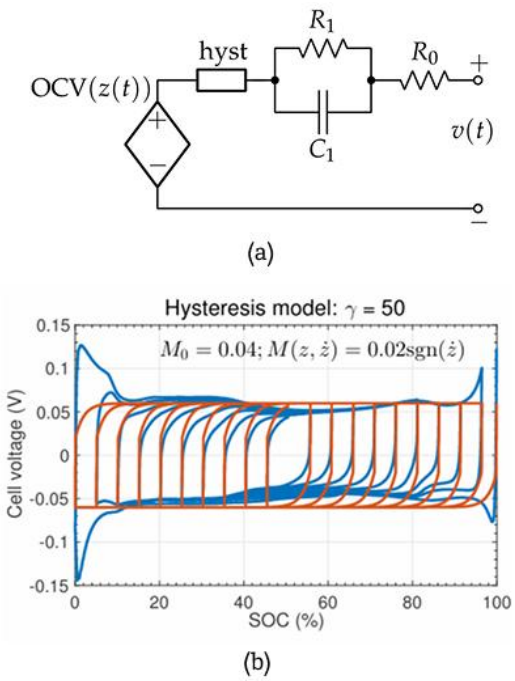

Figure 4. (a) ESC model of a LIB with one RC term (b) Cell voltage deviation from OCV against SOC hysteresis scanning. Blue: Experimental; Orange: ESC model. Adapted from [6]

Hu et al. [7] conducted a comparative study in 2012 on how early integer-order ECM architectures affected three critical metrics, accuracy, generalizability, and computational burden, by varying the number of RC pairs, inclusion of hysteresis states, and structural complexity. Hu showed that the first order RC model is preferred for NMC cells, while the first-order RC model with one-state hysteresis seems to be the best choice for LFP cells. The experiments of Tran [8] showed similar results, whom extended the analysis to LMO and NCA, highlighting the dependence on chemistry in ECM selection for use in BMS.

Nonetheless, lithium-ion battery systems exhibit complex interfacial and transport phenomena, with empirical impedance data revealing non-ideal capacitive slopes in voltage response, depressed semicircles from electrochemical impedance spectroscopy (EIS) Nyquist plot that cannot be reproduced by networks of ideal RC elements without excessive model order (EIS is discussed in 4.2). Having established this limitation, the focus now moves to fractional-order ECMs.

3.1.2 Fractional-order ECMs

Fractional-order models (FOMs) include fractional-order elements that generalizes the typical impedance components found in integer-order ECMs. Instead of assuming ideal

capacitive or diffusive processes with single, well-defined time constants, fractional-order elements allow the impedance to follow a power-law form

$$Z(\omega) \propto (j\omega)^{-\alpha}, \qquad 0 < \alpha < 1$$

with constant α which naturally captures systems possessing distributions of relaxation times.

The constant phase element (CPE) is a widely used fractional-order operator in ECMs, found in 26% of ECMs as per Iurilli et al. [9], replacing ideal capacitors in the previously mentioned circuits to represent non-ideal interfacial behaviour. Alternatively, the semi-circles found in Nyquist plots are often represented by two parallel R-CPE segments, representing the SEI and double-layers at the cathode and anode interface Historically, the CPE has been viewed primarily as an empirical fitting element, because no single physical mechanism can fully explain its behaviour across all frequencies [10]. Using CPEs without physical justification leads to ambiguity in interpretation, thus, future work should be done to ground the use of non-ideal elements for LIBs in physics.

Fractional-order behaviour also emerges from diffusion processes, leading to the use of the classical semi-infinite Warburg impedance $Z_W \propto (j\omega)^{-1/2}$, which arises from the slow Fickian diffusion over time scales in which the diffusion layer does not reach a physical boundary. This form is directly relevant for lithium-ion full cells because, over practically accessible EIS frequencies, both electrolyte and solid-phase diffusion behave as semi-infinite processes. Variants such as the finite-length Warburg with reflective boundaries appear when diffusion is confined, and in the case of full cells, at high SOC when lithium concentration fronts reach particle cores, or near current collectors with spatial constraints [11]. The semi-infinite diffusion and reflective boundary Warburg manifest itself as a $\approx 45°$ line and a near-vertical line respectively [11], as shown in Figure 5. These fractional operators offer compact yet expressive characterisations of transport and interfacial dynamics while leveraging the intrinsic memory and non-local properties of fractional derivatives, capturing ageing and relaxation processes in LIBs. Nonetheless, Warburg impedances cannot

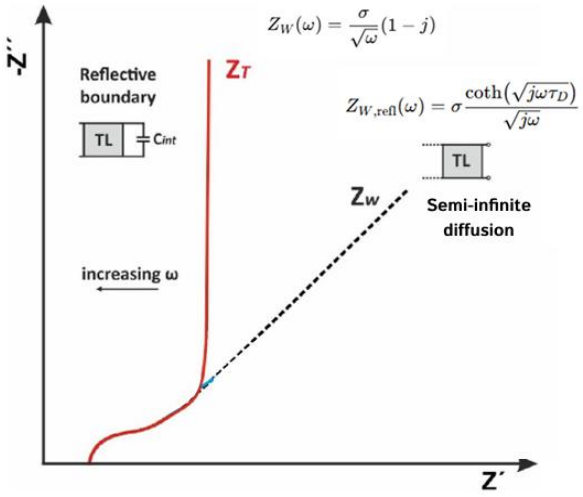

Figure 5. Nyquist plot of LIB from EIS at different mass-transfer regimes. Adapted from [11] with added equations

resolve concentration gradient inside particle, such that the surface concentration and real electrode potential cannot be obtained for improved state estimation [12].

These fractional elements integrate naturally into the Randles circuit, which provides a principled way to represent the distributed and history-dependent electrochemical processes present in LIB electrodes without inflating model order, while remaining compatible with ECM-based estimation and adaptive identification frameworks.

3.1.3 Lumped ECM for Degradation

Tran [13] investigated the effects of SOC, SOH, and temperature on Thevenin ECM parameters in 2021, showing that each parameter exhibits distinct sensitivity, with temperature exerting the strongest influence, SOC primarily affecting the polarization branches, and SOH driving monotonic increases mainly in $R_0$and R_1, alongside corresponding changes in time constants that mirror underlying electrochemical processes; he also developed a three-variable empirical surface model $R_0, R_1, R_2 = f(\mathrm{SOC}, T, \mathrm{SOH})$ that accurately reconstructs ageing-dependent voltage behaviour suitable for real-time BMS implementation. More generally, integer-order ECMs offer practical insights into degradation by linking adaptive parameters to macroscopic performance decay. For instance, ohmic and polarization resistances typically increase over time, quantifying power fade, while the polarization capacitance decreases as LIB ages, serving as a quantifiable indicator of capacity fade. That said, a lumped structure ultimately limits the extent to which degradation modes or mechanistic origins can be resolved.

Cuervo-Reyes et al. [14] proposed an ageing identification method by linking the CPE exponent to ageing. They postulated since “lithium intercalation in the cathode is generally treated as a diffusion process”, representing this process with a CPE in the low-frequency Nyquist tail necessitates “a phase $\theta = -\pi/4$”, and that this value becomes more negative with ageing. They observe an α exponent reduction when the cell is subjected to drive cycles. This proposed link is complicated by the fact that the CPE phase is also susceptible to changes at extreme SOCs, acting as a confounding

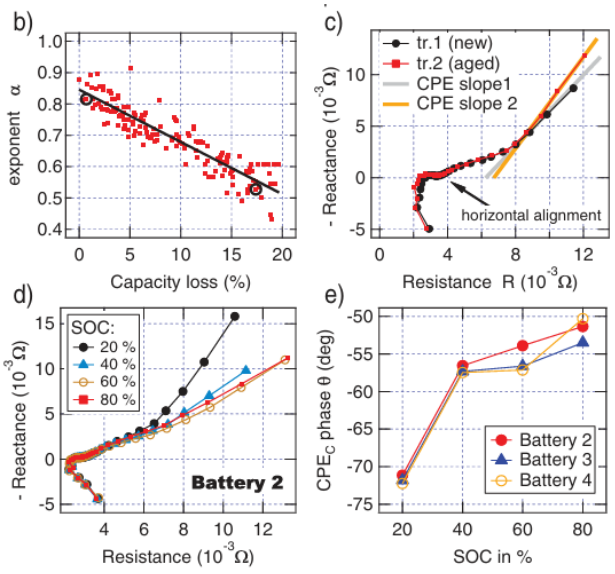

Figure 6. Cathode CPE reaction results a) phase θ of cathode CPE at 60% CPE b) Nyquist plot at different SOC c) Nyquist plot comparison of new (black) and aged (red) cell [14]

variable. While the statement that CPE must have a phase $\theta = -\pi/4$ is an overgeneralization, the paper provided relevant insights of extracting physically meaningful ageing insights from a single component. The relevant graphs are shown in Figure 6.

Similarly, Du et al. 2025 [15] used a 1RC fractional-order ECM with CPEs to represent both the charge transfer and semi-infinite diffusion process, which enables real-time diagnosis onset of lithium plating onset, as shown in Figure 7. By instead of the diffusion tail, they tracked the drop in R_{ct}. When lithium plating occurs, an additional plating-induced charge-transfer resistance emerges and acts in parallel with the existing. This parallel connection causes a reduction in the overall measured charge-transfer resistance. By associating the abnormal drop in R_{ct} with the underlying microscopic degradation process, the model adaptively updates its parameters using dynamic impedance measurements identified through the Nelder–Mead algorithm, while an adaptive statistical threshold, computed from a rolling mean and standard deviation of recent impedance values, adjusts the detection criterion to normal operating fluctuations and thereby mitigates false positives.

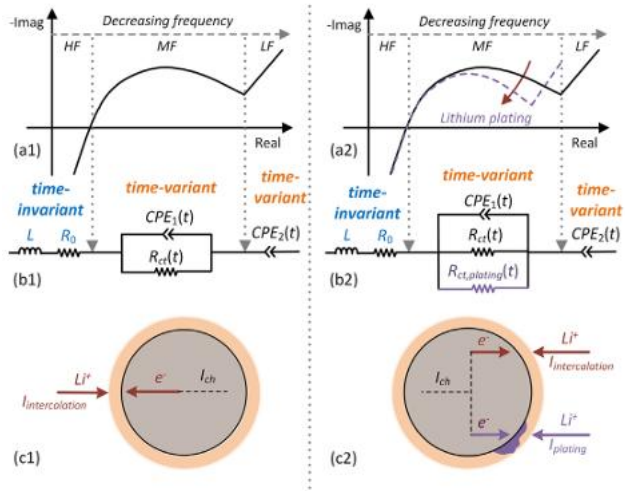

Figure 7. Comparison of 1) normal, and 2) lithium plating conditions during charging: a) Nyquist plots b) ECM units c) Simplified electrochemical processes illustration. Adapted from [15]

Nonetheless, lumped ECMs lack parameters that have one-to-one correspondence to real physical processes, which limits mechanistic interpretability. This is particularly troublesome when attempting to describe degradation, for instance, to model SEI growth and lithium plating over time. PI-ECMs attempt to address this by embedding structural or parametric links to underlying electrochemistry, allowing circuit elements to reflect internal states

3.2 Physics-informed ECM (PI-ECM)

Although physics-informed ECMs have gained substantial traction, the broad and inconsistent definition of PI-ECMs has weakened its utility for analysis. To synthesize the diverse work in this field, I propose a two-class taxonomy reflecting the varying degrees of mechanistic coupling seen across recent research: structurally PI-ECMs, where circuit structure emerges from discretised first-principles models, and parametrically PI-ECMs,

where physics enters through parameter evolution and mechanistic interpretation rather than circuit topology. Following a high-level overview of physics-based models (PBMs), this section discusses these two PI-ECM classes and their implications for degradation analysis.

3.2.1 Overview of Physics-Based Models (PBMs)

Physics-based models (PMBs) provide the mechanistic foundation upon which PI-ECMs are constructed. These models represent the coupled processes governing battery operation. The Doyle-Fuller-Newman (DFN) model, also known as the pseudo-two-dimensional (P2D) model [16], is the most complete representation of porous-electrode behaviour, which is based on the porous electrode theory [17] and concentrated solution theory. The DFN model resolves lithium diffusion within spherical active-material particles using the standard diffusion law that governs how lithium spreads inside solids, and it describes electrolyte concentration by applying the corresponding transport law for ion motion in porous media. Charge conservation is enforced separately in the solid and electrolyte phases by ensuring that all electrical currents entering and leaving each region balance, and the interfacial current density is determined using the Butler–Volmer electrochemical kinetics relation [18].
Figure 8 provides a visual representation of the equations at play.

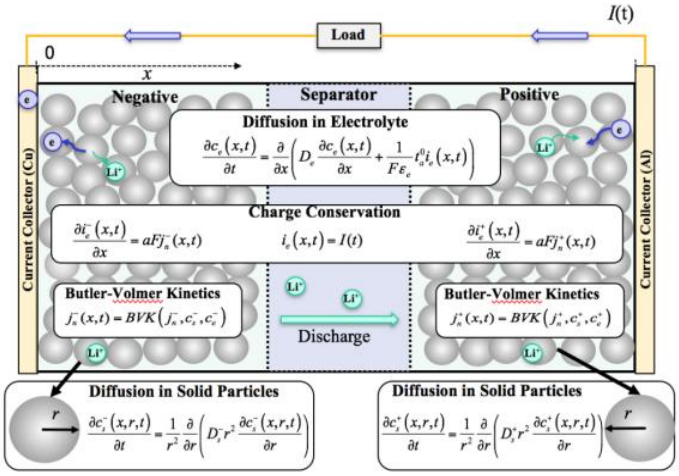

Figure 8. DFN model of LIBs. Source: [18]

It has been emphasised that the DFN model links material-level parameters, such as diffusivities and exchange current densities, to macroscopic performance variables, which makes it an important reference for ECM interpretability [5]. However, solving the coupled nonlinear PDEs in the DFN system requires significant computational effort.

Consequently, the literature shows a “cascade of simplification”, as intuitively described by biju et al. [19] and illustrated in Figure 9. The full DFN model resolves solid diffusion, electrolyte transport, kinetic reactions, and thermal effects in detail, while the SPMeT and SPMe sequentially remove thermal coupling and then simplify electrolyte dynamics into a one-dimensional approximation that still preserves reaction-rate heterogeneity. The SPM

represents the final reduction by modelling each electrode as a single particle and assuming a uniform electrolyte, retaining only solid-phase diffusion and thereby trading physical completeness for computational efficiency [20].

3.2.2 Structurally Physics-Informed ECMs

A structurally physics-informed ECM (henceforth referred to as SPI-ECM) is functionally a **circuit analogue** or network representation of a high-fidelity physicochemical model.

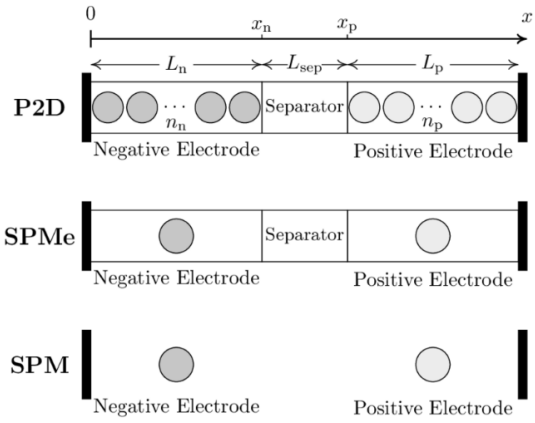

Figure 9. the P2D model, the SPMe and the SPM. Source: [20]

von Srbik et al. [21] presented one of the earliest fully realised SPI-ECMs, recasting the entire DFN model into three coupled distributed networks representing the electronic, ionic and chemical cell domains in Simulink. The three coupled domains are handled by the Triple Species Element (TSE), which enforces conservation laws at every discretized interface. Every circuit element is directly linked to the local electrochemical state, allowing resistances, capacitances, and interfacial overpotentials to evolve naturally with concentration, temperature, and passivating-layer growth yielding a self-updating model driven directly by first principles rather than empirical tuning.

However, its reliance on numerous poorly identifiable physicochemical parameters limits deployability [21]. Merla et al. [22] added that several values are literature assumptions rather than measured quantities, further restricting the model's usability for simulating new cells that have yet been fully parameterized. Besides, the model functions more as a forward simulator than a model suitable for calibration, which fundamentally restricts its use in BMS-type estimation tasks.

By contrast, Merla et al.'s distributed ECM [23] deliberately sacrifices electrochemical completeness for identifiability, requiring only three low-cost experiments (slow discharge, pulse discharge, and EIS). A notable advantage is its explicit encoding of particle-size distributions, enabling mechanistic interpretation of SEI resistance trends with radius and providing a more modular structure. Merla's simulations reproduce expected trends in porosity grading and particle-size uniformity. however, the model inherits the DFN's strong structural assumptions without fully resolving electrolyte or thermal coupling, limiting its robustness under aggressive drive cycles.

In parallel, by modelling the porous electrode as cylindrical particle based on early works by De Levie in the 1960s, Scipioni et al. [23] applied a transmission-line model to a commercial LFP cylindrical cell, modelling the anode and cathode with separate TLMs. Doing so allows reaction distributions along the electrode thickness to emerge naturally from the distributed circuit. Each spatially repeated electrical elements, or “micro units just like building blocks”, as intuitively described by Yang et al. [22, p. 9], contained an equivalent circuit sub-element (ζ), with a Randle’s circuit on the cathode side (Figure 10a) and a Meyer’s element (Figure 10c) on the anode side. It’s also worth noting that the electrical resistance on the anode side is considered negligible, since $R_{el} \ll R_{ion}$, whereas conversely, the cathode side R_{el} is not negligible since lithium-compound cathodes such as LFP must be coated with carbon binders and additives to improve their conduction pathways. This assumption is generally accepted across the literature triaged [23]-[25]. However, since the authors assumed constant ionic and charge-transfer resistances in time, meaning the TLM neglects electrolyte concentration-gradient-driven diffusion and includes only ionic migration, the model is only validated at 0.1C, without any mention of higher-load simulations, nor any linkage to thermal effects and coupled degradation evolution.

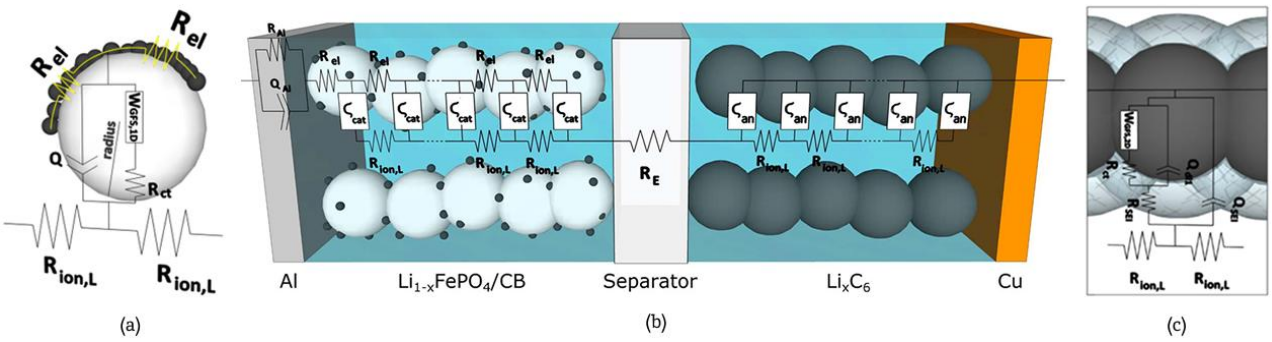

Figure 10. a) Randle's circuit for cathode, b) Full cell ECM proposed by Scipioni et al. c) Meyer's element for anode. Adapted from [23]

Li [26] also derived a physics-based distributed-parameter ECM from the P2D model, using the finite volume method (FVM). The entire ECM is government by ODEs rather than differential algebraic equations, wherein all elements are expressed as explicit functions of state and input variables. Notably, Li introduced an ideal transformer with turns ratio $1:1$ to embody energy conservation between charge-transfer and mass-transfer processes, yet numerous papers suggested its implementation is “not needed” [27], and that it introduces additional complexity and hinders implementation [28].

In 2020, Geng [25] proposed an ECM with a transmission line model (TLM) structure that consists of resistors that vary with concentration (Figure 11). It combined with two partial differential equations for the mass transport processes, which are solved numerically. It

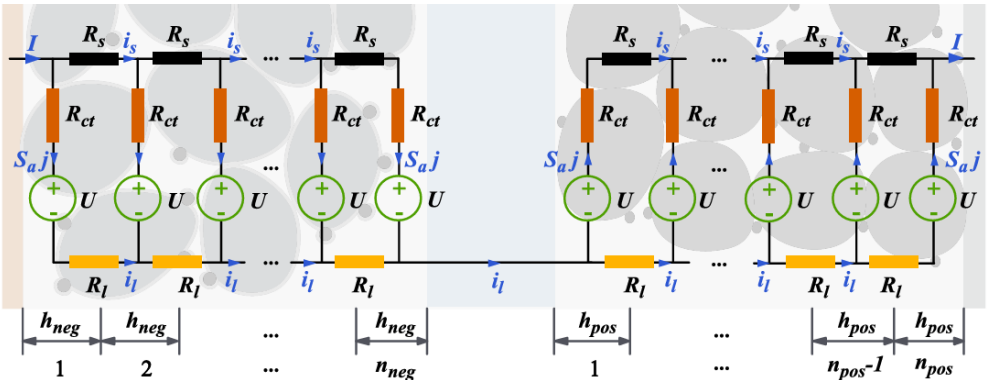

Figure 11. LIB discharge expressed as a TLM. Source: [25]

marked an improvement to the previous models in that no empirical fitting from measured or simulated data is required. It models electronic conduction using a fixed resistor R_s that does not change unless the model is coupled with temperature or ageing. The charge transfer resistance R_{ct} is initialized from a truncated Taylor series of the Butler-Volmer equation, while the electrolyte resistances R_l from the electrolyte conductivity κ, both and updated according to local current density readings and lithium-ion concentrations. The modular mesh offers tunable spatial resolution, with computation time scaling linearly with mesh elements.

Building directly upon Geng's discretised TLM structure, a recent 2025 paper by Wang et al. [29] extends the approach to model incipient degradation mechanisms, specifically SEI growth and metal dendrite formation. Their framework preserves Geng's spatial mesh while introducing additional interfacial and resistive elements representing degradation-driven changes in lithium inventory. Specifically, the charge transfer current density of each TLM segments were further divided into three main reactions, charge transfer current density j_n, SEI growth charge transfer current density J_{SEI} and metal dendrite growth charge transfer current density j_{MD},

$$j = j_n + j_{SEI} + j_{MD}$$

Assuming small SEI and metal dendrite growth current, their respective associated resistances are represented by a linearized form:

$$R_{SEI} = \frac{RT}{i_{SEI} F S_a h} \qquad R_{MD} = \frac{RT}{i_{MD} F S_a h}$$

where h is the element mesh sizing, S_a is the specific surface area, and the rest as previously defined. The parameters are adaptively updated using a genetic algorithm, enabling the model to reproduce ageing voltage behaviour with mean relative error below 0.72%. This branch of TLM development thus moves towards fault-aware and degradation-sensitive circuit representations suitable for health diagnostics.

Although SPI-ECMs inherit their topology from porous-electrode conservation laws, their numerical fidelity still depends strongly on the discretisation scheme. Finite-volume methods (FVMs) enforce conservation and flux continuity by construction, offering superior stability for stiff electrochemical systems where lithium and charge balance are critical. Finite-difference schemes such as Geng et al. [25] are simpler but require stabilisation, and FVM generally remains more robust at high C-rates, under coupled multi-physics, and when extending models to thermal or multidimensional domains.

While models frequently claim to consistently out-perform previously developed models, it appears to have exhibited a contradiction: some SPI-ECMs treats accuracy as its metric and claim to reproduce DFN-level physics with high structural fidelity, while others deliberately collapse this structure to recover identifiability, treating computational efficiency as the performance metric. These divergent design choices highlight that proclaimed “improvements” can be deceiving, and that the intended application, the constraints under which the model is deployed, as well as both computational efficiency and accuracy must be considered in parallel.

3.2.3 Parametrically Physics-Informed ECMs

Parametrically physics-informed ECMs (henceforth referred to as PPI-ECMs) are characterised by classical circuit topologies whose interpretability arises not from their structure but from how their parameters evolve with operating conditions, ageing, or imposed stress. Here, physics enters through parameter evolution rules, mechanistic interpretation, and constraints grounded in electrochemical theory rather than through explicit spatial discretisation as in SPI-ECMs. These models aim to retain the BMS-compatibility of lumped ECMs while capturing some of the mechanistic richness of PBMs.

Barzacchi et al. [31] introduced a method that links electrochemical properties to the parameters of a 2RC ECM for early degradation detection. Using a P2D model as a virtual battery, they varied six degradation-relevant electrochemical parameters, solid diffusivities (D_{sn}, D_{sp}), electrolyte ambipolar diffusivity and conductivity $(\widetilde{D}, \sigma)$, and charge-transfer kinetic constants (i_{00n}, i_{00p}), and quantified their effects on the ECM parameters.

Their analysis showed that electrolyte degradation mainly affects the fast RC branch (R_1, C_1), intercalation-kinetics degradation primarily increases the ohmic resistance R_0, and solid-state diffusion degradation appears in the slow RC branch (R_2, C_2). Because each degradation mode maps to a distinct subset of ECM parameters within a range of characteristic times, the model enables online identification in a BMS.

Mmeka et al. [32] extend parametric PI-ECMs into ageing prognosis by proposing an ageing-sensitive ECM comprising two sets of circuit elements plus a series resistor, where spatially distributed physical degradations are lumped into a small number of interpretable ageing parameters. Their model successfully predicts the onset of the “knee” in the capacity loss curve, a critical event often associated with irreversible lithium plating. Importantly, the model demonstrates that LAM and LLI both increase the ECM’s ageing parameters, creating a positive feedback loop that accelerates degradation. While promising for prognostic tasks, future work should be done to make the model adaptive and applicable for BMS upon validating under diverse drive cycles ensure robustness beyond controlled laboratory conditions.

This approach differs fundamentally from the lumped ECMs discussed in 3.1.3, where parameter changes are observed empirically and lack explicit links to underlying physicochemical processes, in that parametrically physics-informed ECMs enable degradation diagnosis grounded in physical causality rather than purely data-driven trends. This class of models is becoming a key direction for next-generation diagnostic models.

4 Parameter Identification and State Estimation

4.1 Adaptive Algorithms

Combinations of adaptive algorithms alongside empirical data are frequently adopted.

4.1.1 Least Square Family Methods

Least-squares (LS) approaches estimate ECM parameters by minimizing the discrepancy between measured and model predicted voltage. Such deterministic models by definition produce the same output and follow the same sequence of steps in its progression, assuming that the input and initial conditions are unchanging [5]. The batch form computes the optimal parameter vector

$$\hat{\theta}_{LS} = (X^T X)^{-1} X^T Y$$

where X is the regressor matrix and Y is the measurement vector. Because batch LS recomputes all parameters when new data arrive, recursive least squares (RLS) methods are preferred in online state-estimation settings. RLS updates parameters incrementally using previous estimates and measurement, making it well suited for gradual degradation processes. Its lack of complex matrices and low computational power made it a common choice. However, noise-corrupted current and voltage sensors could undermine the robustness of the methods estimations. Wei et al. suggested a novel method for mitigating this issue using a Frisch scheme-based bias compensating RLS, which later evolved into a recursive total least square-based observer [33]. Another limitation of the traditional RLS is that over prolonged periods of time, data saturation may occur due to shrinking of the gain matrix. To account for this effect, forgetting factor is often introduced to adjust the ratio between old and new data, which has been proven effective in improving the accuracy of estimation algorithms [34], [35].

4.1.2 Metaheuristic Algorithms

Deterministic models such as the RLS are prone to be trapped in local minima [36]. Metaheuristic models, which are “high-level, problem-independent algorithmic frameworks that guide other algorithms in exploring solution spaces to find optimal or near-optimal solutions for complex optimization problems” [37, p. 10], attempt to mitigate these challenges by exploring the parameter space stochastically. The graphical abstraction for a particle swarm optimization (PSO) algorithm is presented in Figure 12 as an example.

A 2025 study by Sun et al. [36] systematically compared six common metaheuristic parameter identification methods with the least square method. To ensure a fair assessment, the computational duration for each algorithm was equalized at 3 seconds by adjusting the maximum number of iterations accordingly. The models are tested over various SOC and SOH, using both HPPC and EIS. The results showed that Particle Swarm Optimization (PSO) and Grey Wolf Optimisation (GWO) produced the most accurate parameter fits in complex, noise-sensitive environments. Across all methods, accuracy and robustness declined with decreasing SOH, indicating that ageing intensifies identifiability challenges. Importantly, the relative ranking of algorithms did not vary significantly with SOC or SOH, suggesting that modifying

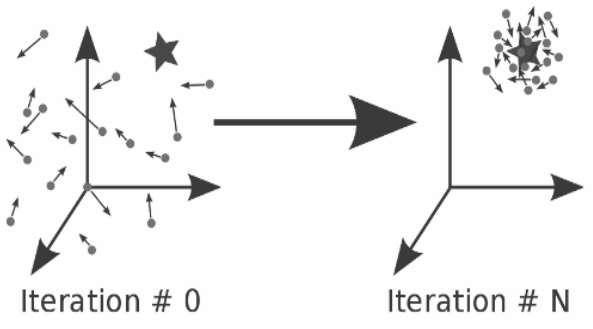

Figure 12. Particle Swarm Optimization (PSO) evolution after N iterations. Source: [45]

parameter identification strategies according to battery state may be unnecessary. It should be noted that the experiments were conducted exclusively NMC cells at $25\ °C$, and that future work should extend the conclusion across a wider temperature range and other chemistries. It's also important to note that, because different metaheuristic algorithms exhibit distinct convergence characteristics, constraining all methods to the same 3-second runtime may bias the comparison.

4.1.3 Kalman Filter Family

The Kalman filter family is a recursive framework used in battery state-estimation, commonly used with the LS or metaheuristic algorithm, using a combination of model predictions and voltage measurements. Extended Kalman Filter (EKF) is a standard state estimation approach that operates on nonlinear systems and sensors and can be used to estimate Li-ion battery states x and parameters θ, by considering both imperfect models and sensors. The prediction and correction steps used to solve the discrete-time state-space equations are shown in Figure 13.

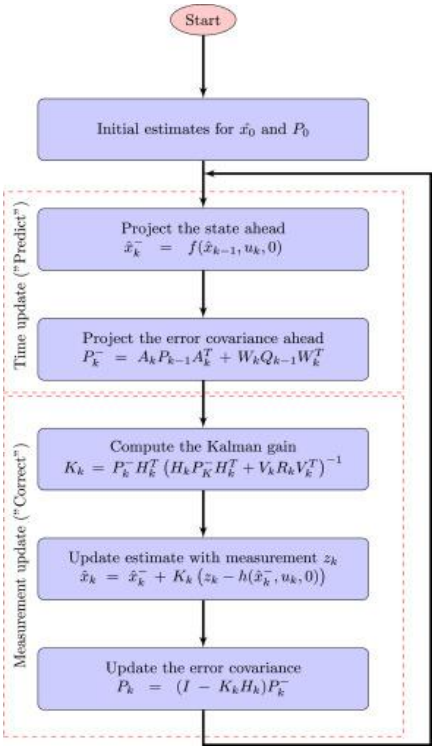

Figure 13. The EKF algorithm. Source: [46]

Plett's 2004 trilogy [38]-[40] established the foundational framework for applying Extended Kalman Filters (EKFs) to lithium-ion battery state estimation, by using first-order Taylor expansion to approximate nonlinear models. Together, the trilogy forms the earliest complete EKF-based BMS framework and remains still the conceptual foundation for virtually all modern SOC or SOH estimation algorithms. EKF remains widely adopted in BMS practice because it achieves a practical balance between accuracy, stability, and computational cost. More advanced variants (e.g., UKF, EnKF [30]) mitigate some shortcomings but at higher computational complexity, making the EKF an effective baseline estimator within real-time battery applications.

4.2 Experimental Identification and Estimations

Experimental methods are commonly applied in an offline setting for parameter and state initialization. Hybrid Pulse Power Characterization (HPPC) and Galvanostatic Intermittent Titration Technique (GITT) are both battery testing techniques used for dynamic parameter estimation, particularly lumped ECMs, but they differ in their approach. While HPPC

applies high-current pulses followed by a rest period, GITT applies constant current pulses with longer relaxation times [41].

Electrochemical impedance spectroscopy (EIS) is another non-invasive impedance-based technique, which involves passing a small AC perturbation across a frequency range, to a cell to characterize interfacial and transport properties. Though historically treated as an offline parameterization tool, EIS is increasingly being exploited for online adaptive identification, as PI-ECMs demand onboard computation of EIS-derived parameters. Recent work shows promising results in such field. Wang et al. [42] proposed in 2023 an adaptive parameter correction strategy based using onboard EIS, from SOC estimation using EKF, and tracked the evolution of the impedance spectrum over accelerated ageing. In the experiment, the BMS is integrated with an analog-front-end (AFE) chip with EIS function, which collects data whenever the battery rest time exceeds the 30-minute threshold and can be assumed quasi-steady. The SOC estimation method is illustrated in Figure 14.

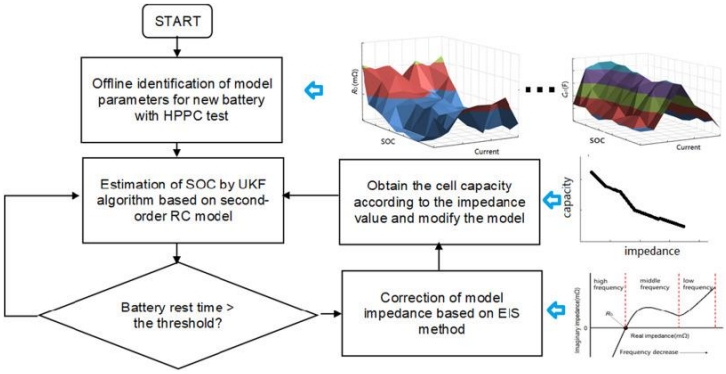

Figure 14. Optimizing EKF-based SOC estimation using onboard EIS

A forthcoming paper by Luo et al. [43] extended this direction by proposing a master–slave architecture in which modular level board acquire impedance data and perform simple reconstruction while a cloud-edge-device framework perform computationally intensive tasks such as Distribution of Relaxation Times (DRT) analysis and physics-based parameter extraction to the cloud, enabling richer diagnostics without overloading the BMS MCU. Keeping the BMS-side workload minimal aligns well with PI-ECM requirements.

This offloading mechanism directly supports the deployment of PI-ECMs, as the cloud can handle nonlinear parameter identification and degradation modelling, while the BMS runs only low-overhead state propagation using periodically updated parameters. However, since deploying traditional EIS requires a depolarised cell, it cannot provide dynamic, in operando, impedance information. This limitation highlights the research priority to develop wideband EIS techniques that capture both low-frequency diffusion and high-frequency connection effects while understanding more about the physical implications when a cell is subjected to dynamic EIS [43].

5 Conclusion

This paper set out to critically evaluate the evolution of adaptive lithium-ion battery equivalent circuit modelling for degradation-aware modelling in BMS. The review confirms that lumped ECM remain dominant in practical BMS implementations due to their robustness and low computational cost. Fractional-order elements such as the CPE, remain weakly interpretable from a physical standpoint, indicating a need for further work to establish their validity beyond impedance fitting. To better capture the breadth and intent of developments a new taxonomy for physics-informed ECM was proposed, distinguishing between parametrically physics-informed (PPI) and structurally physics-informed (SPI) approaches, enabling a more focused synthesis of the literature.

SPI-ECMs derived from DFN formulations demonstrate clear improvements in physical causality and spatial resolution, efficient parameterization remains an issue for use in a BMS. While advances in adaptive algorithms and experimental techniques such as on-board EIS may enable future breakthroughs in this class, PPI-ECMs currently emerge as the most attractive and actively developing approach.

Both PPI-ECMs and SPI-ECMs attempted to directly associate circuit parameters with electrochemical phenomena related to SEI growth, lithium plating, and dendrite formation. However, no ECMs were identified that are structurally capable of capturing degradation mechanisms such as particle cracking, as extracting micro-scale mechanical information from impedance data alone is inherently challenging. This suggests that complementary diagnostic techniques, including ultrasound imaging and additional sensor fusion, may be more suitable for this purpose [44].

Finally, ECM suitability is strongly dependent on the intended BMS functions, sensing capabilities, and embedded computational constraints, which collectively determine discretisation strategy, model fidelity, and the extent of physical coupling that can be supported in real time. Meaningful comparison in an application-agnostic manner remains difficult. Future work should therefore evaluate models against explicit BMS deployment contexts, positioning function and architecture-aware assessment as a prerequisite for degradation-aware model selection.

References

[1] Edge, O'Kane, "Lithium ion battery degradation: what you need to know," *Phys. Chem. Chem. Phys.,* vol. 23, *(14),* pp. 8200–8221, 2021. Available: http://dx.doi.org/10.1039/D1CP00359C. DOI: 10.1039/D1CP00359C.

[2] Doyle, Fuller, "Modeling of Galvanostatic Charge and Discharge of the Lithium/Polymer/Insertion Cell," *J. Electrochem. Soc.,* vol. 140, *(6),* pp. 1526, 1993. Available: https://doi.org/10.1149/1.2221597. DOI: 10.1149/1.2221597.

[3] Hua, Zhang, "Finding a better fit for lithium ion batteries: A simple, novel, load dependent, modified equivalent circuit model and parameterization method," *J. Power Sources,* vol. 484, pp. 229117, 2021. .

[4] Hu, Li, "A comparative study of equivalent circuit models for Li-ion batteries," *J. Power Sources,* vol. 198, pp. 359–367, 2012. Available: https://www.sciencedirect.com/science/article/pii/S0378775311019628. DOI: 10.1016/j.jpowsour.2011.10.013.

[5] Zheng, Deng, "A comprehensive review of lithium-ion battery modelling research and prospects: in-depth analysis of current research and future directions," *Appl. Energy,* vol. 401, pp. 126688, 2025. Available: https://www.sciencedirect.com/science/article/pii/S0306261925014187. DOI: 10.1016/j.apenergy.2025.126688.

[6] Plett*Battery Management Systems, Volume II: Equivalent-Circuit Methods.* 2015Available: https://ieeexplore.ieee.org/servlet/opac?bknumber=9100098.

[7] X. Hu, H. Yuan, "Co-Estimation of State of Charge and State of Health for Lithium-Ion Batteries Based on Fractional-Order Calculus," *IEEE Transactions on Vehicular Technology,* vol. 67, *(11),* pp. 10319–10329, 2018. . DOI: 10.1109/TVT.2018.2865664.

[8] Tran, DaCosta, "Comparative Study of Equivalent Circuit Models Performance in Four Common Lithium-Ion Batteries: LFP, NMC, LMO, NCA," *Batteries,* vol. 7, *(3),* 2021. . DOI: 10.3390/batteries7030051.

[9] Iurilli, Brivio, "On the use of electrochemical impedance spectroscopy to characterize and model the aging phenomena of lithium-ion batteries: a critical review," *J. Power Sources,* vol. 505, pp. 229860, 2021. Available: https://www.sciencedirect.com/science/article/pii/S0378775321003992. DOI: 10.1016/j.jpowsour.2021.229860.

[10] Lasia"The Origin of the Constant Phase Element," *J. Phys. Chem. Lett.,* vol. 13, *(2),* pp. 580–589, 2022. Available: https://doi.org/10.1021/acs.jpclett.1c03782. DOI: 10.1021/acs.jpclett.1c03782.

[11] Lazanas and Prodromidis, "Electrochemical Impedance Spectroscopy—A Tutorial," *ACS Meas. Sci. Au,* vol. 3, *(3),* pp. 162–193, 2023. Available: https://doi.org/10.1021/acsmeasuresciau.2c00070. DOI: 10.1021/acsmeasuresciau.2c00070.

[12] Zhuo, Kirkaldy, "Diffusion-aware voltage source: An equivalent circuit network to resolve lithium concentration gradients in active particles," *Appl. Energy,* vol. 339, pp. 121004, 2023. Available: https://www.sciencedirect.com/science/article/pii/S0306261923003689. DOI: 10.1016/j.apenergy.2023.121004.

[13] Tran, Mathew, "A comprehensive equivalent circuit model for lithium-ion batteries, incorporating the effects of state of health, state of charge, and temperature on model parameters," *Journal of Energy Storage,* vol. 43, pp. 103252, 2021. Available: https://www.sciencedirect.com/science/article/pii/S2352152X2100949X. DOI: 10.1016/j.est.2021.103252.

[14] Cuervo-Reyes, Scheller, "A Unifying View of the Constant-Phase-Element and Its Role as an Aging Indicator for Li-Ion Batteries," *J. Electrochem. Soc.,* vol. 162, *(8),* pp. A1585, 2015. Available: https://doi.org/10.1149/2.0791508jes. DOI: 10.1149/2.0791508jes.

[15] Du, Meng, "Real-time lithium plating onset detection for lithium-ion batteries via dynamic impedance spectra analysis," *Appl. Energy,* vol. 402, pp. 126810, 2025. Available: https://www.sciencedirect.com/science/article/pii/S0306261925015405. DOI: 10.1016/j.apenergy.2025.126810.

[16] Doyle, Meyers, "Computer simulations of the impedance response of lithium rechargeable batteries," *J. Electrochem. Soc.,* vol. 147, *(1),* pp. 99–110, 2000. Available: https://www.scopus.com/inward/record.uri?eid=2-s2.0-0033873550&doi=10.1149%2f1.1393162&partnerID=40&md5=1d3d1dd69036d9ae8164128c09d221ba. DOI: 10.1149/1.1393162.

[17] Newman and Tiedemann, "Porous-electrode theory with battery applications," *AIChE J.,* vol. 21, *(1),* pp. 25–41, 1975. Available: https://www.scopus.com/inward/record.uri?eid=2-s2.0-0016434761&doi=10.1002%2faic.690210103&partnerID=40&md5=66210b9cb2f09f6e38b0c2b0b54cf9a6. DOI: 10.1002/aic.690210103.

[18] He, Pecht, "A Physics-Based Electrochemical Model for Lithium-Ion Battery State-of-Charge Estimation Solved by an Optimised Projection-Based Method and Moving-Window Filtering," *Energies,* vol. 11, *(8),* 2018. . DOI: 10.3390/en11082120.

[19] Biju and Fang, "BattX: An equivalent circuit model for lithium-ion batteries over broad current ranges," *Appl. Energy,* vol. 339, pp. 120905, 2023. Available: https://www.sciencedirect.com/science/article/pii/S0306261923002696. DOI: 10.1016/j.apenergy.2023.120905.

[20] Ai and Liu, "Improving the convergence rate of Newman's battery model using 2nd order finite element method," *Journal of Energy Storage,* vol. 67, pp. 107512, 2023. Available: https://dx.doi.org/10.1016/j.est.2023.107512. DOI: 10.1016/j.est.2023.107512.

[21] von Srbik, Marinescu, "A physically meaningful equivalent circuit network model of a lithium-ion battery accounting for local electrochemical and thermal behaviour, variable double layer capacitance and degradation," *J. Power Sources,* vol. 325, pp. 171–184, 2016. Available: https://www-sciencedirect-com.iclibezp1.cc.ic.ac.uk/science/article/pii/S0378775316305973. DOI: 10.1016/j.jpowsour.2016.05.051.

[22] Merla, Wu, "An easy-to-parameterise physics-informed battery model and its application towards lithium-ion battery cell design, diagnosis, and degradation," *J. Power Sources,* vol. 384, pp. 66–79, 2018. Available: https://www.sciencedirect.com/science/article/pii/S0378775318301861. DOI: 10.1016/j.jpowsour.2018.02.065.

[23] Scipioni, Jørgensen, "A Physically-Based Equivalent Circuit Model for the Impedance of a LiFePO4/Graphite 26650 Cylindrical Cell," *J. Electrochem. Soc.,* vol. 164, *(9),* pp. A2017, 2017. Available: https://doi.org/10.1149/2.1071709jes. DOI: 10.1149/2.1071709jes.

[24] Bihn, Rinner, "Physics-Based Equivalent Circuit Model Motivated by the Doyle–Fuller–Newman Model," *Batteries,* vol. 10, *(9),* 2024. . DOI: 10.3390/batteries10090314.

[25] Geng, Wang, "Bridging physics-based and equivalent circuit models for lithium-ion batteries," *Electrochim. Acta,* vol. 372, pp. 137829, 2021. Available: https://www.sciencedirect.com/science/article/pii/S0013468621001183. DOI: 10.1016/j.electacta.2021.137829.

[26] Li, Vilathgamuwa, "Development of a degradation-conscious physics-based lithium-ion battery model for use in power system planning studies," *Appl. Energy,* vol. 248, pp. 512–525, 2019. Available: https://www-sciencedirect-com.iclibezp1.cc.ic.ac.uk/science/article/pii/S0306261919308049. DOI: 10.1016/j.apenergy.2019.04.143.

[27] Kono, Suzuki, "Physics-Based Circuit Simulation Model of Lithium-Ion Batteries for Model-Based Design of Electrochemical Energy Storage Systems," *IEEJ Journal of Industry Applications,* vol. 14, *(6),* pp. 1088–1100, 2025. Available: https://www.scopus.com/inward/record.uri?eid=2-s2.0-105020377429&doi=10.1541%2fieejjia.25004005&partnerID=40&md5=27396e2d0ad448563a21fdad19863a6b. DOI: 10.1541/ieejjia.25004005.

[28] Graule, Oehler, "Development and Evaluation of a Physicochemical Equivalent Circuit Model for Lithium-Ion Batteries," *J. Electrochem. Soc.,* vol. 171, *(2),* 2024. Available: https://www.scopus.com/inward/record.uri?eid=2-s2.0-85184995558&doi=10.1149%2F1945-7111%2Fad1ec7&partnerID=40&md5=4bed51ab2a6aba9223d77da9340891f9. DOI: 10.1149/1945-7111/ad1ec7.

[29] Z. Wang and M. -Y. Chow, "Battery modeling of SEI and metal dendrite growth: A transmission line circuit framework with genetic algorithm-identified parameters," in *2025 IEEE 20th Conference on Industrial Electronics and Applications (ICIEA),* 2025, . DOI: 10.1109/ICIEA65512.2025.11149030.

[30] Li, Xiong, "Constrained Ensemble Kalman Filter for Distributed Electrochemical State Estimation of Lithium-Ion Batteries," *IEEE Transactions on Industrial Informatics,* vol. 17, *(1),* pp. 240–250, 2021. Available: https://www.scopus.com/inward/record.uri?eid=2-s2.0-85087523475&doi=10.1109%2fTII.2020.2974907&partnerID=40&md5=262a0bb5fb2c21bd0e04d02e327bce70. DOI: 10.1109/TII.2020.2974907.

[31] Barzacchi, Lagnoni, "Enabling early detection of lithium-ion battery degradation by linking electrochemical properties to equivalent circuit model parameters," *Journal of Energy Storage,* vol. 50, pp. 104213, 2022. Available: https://www.sciencedirect.com/science/article/pii/S2352152X22002444. DOI: 10.1016/j.est.2022.104213.

[32] Mmeka, Dubarry, "Physics-Informed Aging-Sensitive Equivalent Circuit Model for Predicting the Knee in Lithium-Ion Batteries," *J. Electrochem. Soc.,* vol. 172, *(8),* 2025. Available: http://dx.doi.org/10.1149/1945-7111/adf9cb. DOI: 10.1149/1945-7111/adf9cb.

[33] Z. Wei, C. Zou, "Online Model Identification and State-of-Charge Estimate for Lithium-Ion Battery With a Recursive Total Least Squares-Based Observer," *IEEE Transactions on Industrial Electronics,* vol. 65, *(2),* pp. 1336–1346, 2018. . DOI: 10.1109/TIE.2017.2736480.

[34] Duong, Bastawrous, "Online state of charge and model parameters estimation of the LiFePO4 battery in electric vehicles using multiple adaptive forgetting factors recursive least-squares," *J. Power Sources,* vol. 296, pp. 215–224, 2015. Available: https://www.sciencedirect.com/science/article/pii/S0378775315300884. DOI: 10.1016/j.jpowsour.2015.07.041.

[35] He, Zhang, "Online model-based estimation of state-of-charge and open-circuit voltage of lithium-ion batteries in electric vehicles," *Energy,* vol. 39, *(1),* pp. 310–318, 2012. Available: https://www.sciencedirect.com/science/article/pii/S036054421200014X. DOI: 10.1016/j.energy.2012.01.009.

[36] Sun, Liu, "A comparative study of parameter identification methods for equivalent circuit models for lithium-ion batteries and their application to state of health estimation," *Journal of Energy Storage,* vol. 114, pp. 115707, 2025. Available: https://www.sciencedirect.com/science/article/pii/S2352152X25004207. DOI: 10.1016/j.est.2025.115707.

[37] Pour Haji Kazem"Chapter 2 - artificial intelligent algorithms, motivation, and terminology," in *Decision-Making Models*, Allahviranloo, Pedrycz, Eds. 2024, Available: https://www.sciencedirect.com/science/article/pii/B978044316147600030X. DOI: 10.1016/B978-0-443-16147-6.00030-X.

[38] Plett"Extended Kalman filtering for battery management systems of LiPB-based HEV battery packs: Part 1. Background," *J. Power Sources,* vol. 134, *(2),* pp. 252–261, 2004. Available: https://www.sciencedirect.com/science/article/pii/S0378775304003593. DOI: 10.1016/j.jpowsour.2004.02.031.

[39] Plett"Extended Kalman filtering for battery management systems of LiPB-based HEV battery packs: Part 2. Modeling and identification," *J. Power Sources,* vol. 134, *(2),* pp. 262–276, 2004. Available: https://www.sciencedirect.com/science/article/pii/S037877530400360X. DOI: 10.1016/j.jpowsour.2004.02.032.

[40] Plett"Extended Kalman filtering for battery management systems of LiPB-based HEV battery packs: Part 3. State and parameter estimation," *J. Power Sources,* vol. 134, *(2),* pp. 277–292, 2004. Available: https://www.sciencedirect.com/science/article/pii/S0378775304003611. DOI: 10.1016/j.jpowsour.2004.02.033.

[41] Samieian, Hales, "A Novel Experimental Technique for Use in Fast Parameterisation of Equivalent Circuit Models for Lithium-Ion Batteries," *Batteries,* vol. 8, *(9),* 2022. . DOI: 10.3390/batteries8090125.

[42] Wang, Zhao, "Application of electrochemical impedance spectroscopy in battery management system: State of charge estimation for aging batteries," *Journal of Energy Storage,* vol. 57, pp. 106275, 2023.

Available: https://www.sciencedirect.com/science/article/pii/S2352152X22022642. DOI: 10.1016/j.est.2022.106275.

[43] Luo, Gao, "A review of on-board electrochemical impedance spectroscopy for low-cost in situ characterization technology," *Journal of Energy Storage,* vol. 141, pp. 119153, 2026. Available: https://www.sciencedirect.com/science/article/pii/S2352152X25038666. DOI: 10.1016/j.est.2025.119153.

[44] Yang, Mao, "Recent advances in ultrasound-based battery diagnostics: A reinforcement learning perspective," *Sustainable Energy Technologies and Assessments,* vol. 82, pp. 104521, 2025. Available: https://www.sciencedirect.com/science/article/pii/S2213138825003522. DOI: 10.1016/j.seta.2025.104521.

[45] ESA Pagmo2. *Particle Swarm Optimization (PSO)*. Available: https://esa.github.io/pagmo2/docs/cpp/algorithms/pso.html.

[46] Mohamed, Yu, "Advancements in parameter estimation techniques for 1RC and 2RC equivalent circuit models of lithium-ion batteries: A comprehensive review," *Journal of Energy Storage,* vol. 113, pp. 115581, 2025. Available: https://www.sciencedirect.com/science/article/pii/S2352152X25002944. DOI: 10.1016/j.est.2025.115581.